Observability Analysis of a Power System Stochastic Dynamic Model Using a Derivative-Free Approach

Zongsheng Zheng , Member, IEEE, Yijun Xu, Senior Member, IEEE, Lamine Mili, Life Fellow, IEEE, Zhigang Liu, Senior Member, IEEE, Mert Korkali, Senior Member, IEEE, and Yuhong Wang, Member, IEEE

Abstract—Serving as a prerequisite to power system dynamic state estimation, the observability analysis of a power system dynamic model has recently attracted the attention of many power engineers. However, because this model is typically nonlinear and large-scale, the analysis of its observability is a challenge to the traditional derivative-based methods. Indeed, the linearapproximation-based approach may provide unreliable results while the nonlinear-technique-based approach inevitably faces extremely complicated derivations. Furthermore, because power systems are intrinsically stochastic, the traditional deterministic approaches may lead to inaccurate observability analyses. Facing these challenges, we propose a novel polynomial-chaos-based derivative-free observability analysis approach that not only is free of any linear approximations, but also accounts for the stochasticity of the dynamic model while bringing a low implementation complexity. Furthermore, this approach enables us to quantify the degree of observability of a stochastic model, what conventional deterministic methods cannot do. The excellent performance of the proposed method has been demonstrated by performing extensive simulations using a synchronous generator model with IEEE-DC1A exciter and the TGOV1 turbine governor.

Index Terms—Dynamic state estimation, observability analysis, derivative-free, polynomial chaos, degree of observability.

I. INTRODUCTION

YNAMIC state estimation (DSE) has attracted an increasing attention of power engineers due to its ability to enhance the monitoring, stability, and control of power systems. Several applications of DSE in power systems have been

Manuscript received December 6, 2020; revised April 5, 2021; accepted May 9, 2021. Date of publication May 13, 2021; date of current version October 20, 2021. This work was supported in part by the Scientific Research Startup Fund for Introducing Talents of Sichuan University under Grant 1082204112576, in part by the U.S. NSF Grant 1917308 and in part by the U.S. DOE Office of Electricity Advanced Grid Modeling Program, and performed under the auspices of the U.S. DOE by LLNL under Contract DE-AC52-07NA27344. Document released as LLNL-JRNL-817371. Paper no. TPWRS-01996-2020. (Corresponding author: Yijun Xu.)

Zongsheng Zheng and Yuhong Wang are with the College of Electrical Engineering, Sichuan University, Chengdu 610065, China (e-mail: zongsheng56@126.com; yuhongwang@scu.edu.cn).

Yijun Xu and Lamine Mili are with the Bradley Department of Electrical and Computer Engineering, Virginia Tech, Northern Virginia Center, Falls Church, VA 22043 USA (e-mail: xuyijun2012app@gmail.com; lmili@vt.edu).

Zhigang Liu is with the School of Electrical Engineering, Southwest Jiaotong University, Chengdu 610031, China (e-mail: liuzg_cd@126.com).

Mert Korkali is with the Computational Engineering Division, Lawrence Livermore National Laboratory, Livermore, CA 94550 USA (e-mail: korkali1@llnl.gov).

Color versions of one or more figures in this article are available at https://doi.org/10.1109/TPWRS.2021.3079919.

Digital Object Identifier 10.1109/TPWRS.2021.3079919

proposed in the literature [1]–[8]. A prerequisite to the power system state estimation is the observability of that system by a collection of measurements. Observability analysis aims at evaluating the existence of a solution for the state estimation problem, and thereby at providing guidelines to sensor deployment, measurement selection, and so on, for achieving reliable state estimation results. Since an actual power system is nonlinear, large-scale, and time-varying, its observability analysis becomes quite challenging.

To achieve this task, methods based on linear approximations have been initially proposed. Albeit simple, they may suffer from inaccurate or even incorrect results when the system nonlinearities are strong. Therefore, some alternative approaches have been proposed recently in the literature. For instance, Qi et al. [9] apply the empirical observability Gramian for phasor measurement unit (PMU) placement. Although being a computable tool, the approximated constant-impedance load models for a reduced-order system can reduce the accuracy of the analysis result. Wang et al. [10] advocate the application of a Lie-derivative-based observability analysis method to power systems where the synchronous generators are represented by the classical model. This work has been improved by Rouhani and Abur [11] with the use of a more realistic synchronous generator model provided with the IEEE-Type 1 exciter. Albeit accurate under nonlinear conditions, this approach is known to be complicated due to derivatives and very time-consuming even for small-scale power systems. Here, we would like to point out that all the above observability analysis methods are formulated within a deterministic dynamical system model framework without considering the inherent stochasticity of any actual power

To address the aforementioned challenges, we propose in this paper a novel method that relies on the generalized-polynomial-chaos (gPC) theory, which enables reliable observability analysis of a power system stochastic dynamic model. This yields the following contributions:

- 1) Unlike the traditional linear-approximation-based methods, the proposed method applies to nonlinear power system model.
- 2) In contrast to the derivative-involved Lie derivative method, the proposed gPC-based method is fully *derivative-free*, which greatly reduces the derivative complexity and computational burden.
- 3) Unlike the deterministic observability analysis methods proposed in the literature, the proposed method accounts for the

 $0885\text{-}8950 \circledcirc 2021 \text{ IEEE. Personal use is permitted, but republication/redistribution requires \text{ IEEE permission.}} \\ \text{See https://www.ieee.org/publications/rights/index.html for more information.} \\$

stochasticities of the power system. Furthermore, the degree of the system observability is assessed via the index of the *puny* and *brawny* observability by which the proposed approach can not only analyze the observability of each system state, but can also assess the effect of the observation noise on the system observability.

4) Finally, to ensure a better practical observability analysis, our proposed method is applied to the decentralized and centralized DSE frameworks. Its exceptional performance is demonstrated in various simulations using a ninth-order synchronous generator model with the IEEE-DC1A exciter and the TGOV1 turbine-governor [12].

II. PROBLEM FORMULATION

Here, let us first review the conventional deterministic observability analysis framework of a time-varying dynamical system. Then, we extend this framework to the power system dynamic model. Finally, we discuss its limitation and we propose our new gPC-based observability analysis method for a stochastic dynamic model.

A. Review of Observability

Consider a general discrete-time dynamical system formulated as

$$\boldsymbol{x}_{k+1} = \boldsymbol{f}(\boldsymbol{x}_k), \tag{1a}$$

$$\mathbf{y}_k = \mathbf{h}(\mathbf{x}_k),\tag{1b}$$

where $x_k \in \mathbb{R}^{n \times 1}$ and $y_k \in \mathbb{R}^{m \times 1}$ are the state and the measurement vectors at time k, respectively; and f and h are vector-valued functions.

Definition 1: The system is (locally) observable in the time interval [0, K] if the initial state x_0 can be uniquely determined from $y_k, k \in [0, K]$.

Defining the cumulative measurement vector $\boldsymbol{Y}_k = [\boldsymbol{y}_k, \boldsymbol{y}_{k+1}, \dots, \boldsymbol{y}_{k+n-1}]^\mathsf{T}$, the relation between the arbitrary initial state \boldsymbol{x}_k and its corresponding measurements \boldsymbol{Y}_k is given by

$$\boldsymbol{Y}_k = \boldsymbol{g}(\boldsymbol{x}_k). \tag{2}$$

According to the implicit function theorem [13], the initial state x_k can be uniquely determined from the measurements Y_k if and only if the Jacobian matrix

$$O_k = \frac{\partial Y_k}{\partial x_k} \tag{3}$$

is nonsingular. Consequently, the observability rank condition is described as follows:

Theorem 1 [14]: The system (1) is (locally) observable if and only if the Jacobian matrix (also called the observability matrix) has full rank, i.e., $rank(O_k) = n$.

Its state-measurement relation (2) can be represented by

$$\boldsymbol{Y}_k = [\boldsymbol{h}(\boldsymbol{x}_k), \boldsymbol{h}(\boldsymbol{f}(\boldsymbol{x}_k)), \boldsymbol{h}(\boldsymbol{f}(\boldsymbol{f}(\boldsymbol{x}_k))), \dots]^{\mathsf{T}},$$
 (4)

and the corresponding observability is computed through

$$O_k = \left[\frac{\partial h(x_k)}{\partial x_k}, \frac{\partial h(f(x_k))}{\partial x_k}, \frac{\partial h(f(f(x_k)))}{\partial x_k}, \dots \right]^{\mathsf{T}}. \quad (5)$$

Obviously, the derivation procedure within (5) can be complicated for nonlinear and high-dimensional dynamical systems.

B. Power System Dynamics

The discrete-time state-space model of the power system is given by

$$\boldsymbol{x}_{k+1} = \boldsymbol{f}(\boldsymbol{x}_k) + \boldsymbol{w}_k, \tag{6a}$$

$$\boldsymbol{y}_k = \boldsymbol{h}(\boldsymbol{x}_k) + \boldsymbol{v}_k, \tag{6b}$$

where w_k and v_k are the process and measurement noise, respectively. In this paper, following Sauer and Pai [12], the synchronous generator with the IEEE-DC1A exciter and the TGOV1 turbine-governor is modeled by the following differential and algebraic equations:

Differential equations:

$$T'_{d_0} \frac{dE'_q}{dt} = -E'_q - (X_d - X'_d)I_d + E_{fd}, \tag{7}$$

$$T'_{q_0} \frac{dE'_d}{dt} = -E'_d - (X_q - X'_q)I_q, \tag{8}$$

$$\frac{\mathrm{d}\delta}{\mathrm{d}t} = \omega - \omega_s,\tag{9}$$

$$\frac{2H}{\omega_s} \frac{\mathrm{d}\omega}{\mathrm{d}t} = T_M - P_e - D(\omega - \omega_s),\tag{10}$$

$$T_E \frac{\mathrm{d}E_{fd}}{\mathrm{d}t} = -(K_E + S_E(E_{fd}))E_{fd} + V_R,$$
 (11)

$$T_F \frac{dV_F}{dt} = -V_F + \frac{K_F}{T_E} V_R - \frac{K_F}{T_E} (K_E + S_E(E_{fd})) E_{fd},$$
(12)

$$T_A \frac{dV_R}{dt} = -V_R + K_A (V_{\text{ref}} - V_F - V),$$
 (13)

$$T_{CH}\frac{\mathrm{d}T_M}{\mathrm{d}t} = -T_M + P_{SV},\tag{14}$$

$$T_{SV}\frac{\mathrm{d}P_{SV}}{\mathrm{d}t} = -P_{SV} + P_C - \frac{1}{R_D} \left(\frac{\omega}{\omega_s} - 1\right),\tag{15}$$

Algebraic equations:

$$V_d = V\sin(\delta - \theta)$$
 and $V_q = V\cos(\delta - \theta)$, (16)

$$I_d = \frac{E'_q - V_q}{X'_d}$$
 and $I_q = \frac{V_d - E'_d}{X'_q}$, (17)

$$P_e = V_d I_d + V_q I_q$$
 and $Q_e = -V_d I_q + V_q I_d$, (18)

where δ and ω are generator rotor angle and speed, respectively; ω_s is the rotor speed base value; T'_{d_0} , T'_{q_0} , T_E , T_F , T_A , T_{CH} , and T_{SV} are the time constants; K_E , K_F and K_A are the controller gains; E'_d , E'_q , E_{fd} , V_F , V_R , T_M , and P_{SV} are the d- and q-axis transient voltages, field voltage, scaled output of the stabilizing transformer and scaled output of the amplifier, synchronous machine mechanical torque and steam valve position, respectively;

 X_d, X_d', X_q , and X_q' are the generator parameters; H, D, and R_D are the inertia constant (in seconds), damping ratio and droop, respectively; $V_{\rm ref}$ and P_C are the known references for exciter and speed governor, respectively. V and θ are the terminal bus voltage magnitude and phase angle, respectively; I_d and I_q are the d- and q-axis currents; V_d and V_q are the d- and q-axis voltage magnitude; P_e and Q_e are the generator terminal real and reactive power, respectively. The reader is referred to [15] for further details.

By using a time discretization via the fourth-order Runge-Kutta method, the continuous-time state-space model (7)–(18) is written in a discrete-time form given by (6). The relationships given by (7)–(15) and (16)–(18) are represented in compact forms by the vector-valued functions f and h, respectively.

C. Limitations of the Traditional Observability Analysis

Here, let us discuss the limitations of the aforementioned observability analysis. First, since multiple derivatives are involved in the observability analysis, the current approach is very time-consuming even for small-scale power systems. Second, although the current approach assesses the observability of a system as a whole, it does not precisely assess the observability for each system state individually. In some practical applications, ensuring the observability for all the system states may not be necessary since only some key system states really do matter. Finally, the current observability analysis is formulated within a deterministic framework that fully ignores the stochastic nature of a dynamical system such as a power system. Therefore, it comes as no surprise that this deterministic framework lacks relevance in power system applications, where the observation noise cannot be ignored.

Motivated by the above shortcomings, we propose a new observability framework that not only accounts for the stochasticity of the model, but also assesses the observability for each system state and quantifies the degree of observability of the model.

III. REVIEW OF THE POLYNOMIAL CHAOS

Before we present our gPC-based observability analysis, let us have a brief review of the gPC theory first.

A. gPC Surrogate

The gPC theory, which is first introduced by Wiener and further developed by Xiu and Karniadakis [16], has been demonstrated to lead to cost-effective tools in uncertainty propagation of a nonlinear system model [16], e.g., the power system dynamic model [17]. In this theory, the stochastic outputs are expressed as a weighted sum of orthogonal polynomial chaos basis functions constructed from the probability distribution of the random variables, i.e.,

$$y = \sum_{i=0}^{n_p} a_i \phi_i(\boldsymbol{\xi}), \tag{19}$$

where y is the system output, $\boldsymbol{\xi} = [\xi_1, \xi_2, \dots, \xi_n]$ is a vector of random variables following a standard probability distribution, and its corresponding polynomial chaos basis is $\phi_i(\boldsymbol{\xi})$; a_i is

the *i*th polynomial chaos coefficient; $n_p = (n+p)!/(n!p!) - 1$; and p is the maximum order of the polynomial chaos basis functions. From the polynomial chaos coefficients, the mean and the variance of the output y can be directly obtained as

$$\mu = a_0, \tag{20a}$$

$$\sigma^2 = \sum_{i=1}^{n_p} a_i^2.$$
 (20b)

In practice, to maintain the computational efficiency of the surrogate model, (19), a truncated gPC expansion is typically adopted. Although different truncation strategies exist, considering the scalability and accuracy of the power system model, we propose to select the strategy proposed in [18] to truncate the gPC surrogate as

$$y = a_0 \phi_0 + \sum_{i=1}^n a_i \phi_1(\xi_i) + \sum_{i=1}^n a_{i,i} \phi_2(\xi_i^2),$$
 (21)

where ϕ_0 , $\phi_1(\xi_i)$, and $\phi_2(\xi_i^2)$ represent the zeroth-, first-, and second-order polynomial chaos bases, respectively; and $a_0, a_i, a_{i,i}$ stand for the corresponding polynomial chaos coefficients.

B. Collocation Points

Collocation points (CPs) are a finite sample set of $\xi = [\xi_1, \xi_2, \dots, \xi_n]$ that are chosen to approximate the polynomial chaos coefficients. The elements of the CPs are generated by using the union of the zeros and the roots of one higher-order, one-dimensional polynomial for every random variable. Then, using a tensor product or sparse tensor rule, we can generate multidimensional CPs as described in [16], [18]. Here, for Gaussian random variables, we select Hermite polynomials.

C. Approximation of gPC Coefficients

Here, let us present the way to approximate the gPC coefficients for a general function,

$$y = q(x), \tag{22}$$

where the input variable is $\boldsymbol{x} \in \mathbb{R}^{n \times 1}$, and the output variable is $\boldsymbol{y} \in \mathbb{R}^{L \times 1}$. To achieve the surrogate model, the coefficients of gPC are estimated at selected combinations of the aforementioned collocation points, $\boldsymbol{\xi}$. Taking into consideration S independent combinations of the collocation points, the polynomial chaos basis can be obtained directly, and the output variable can be calculated through the considered function (22). Formally, the surrogate model is given by

$$Y = HA, (23)$$

where $\boldsymbol{Y} \in \mathbb{R}^{S \times L}$ is the output matrix consisting of the outputs from S samples; $\boldsymbol{H} \in \mathbb{R}^{S \times (2n+1)}$ is the basis matrix composed

of the polynomial chaos bases expressed as

$$\boldsymbol{H} = \begin{bmatrix} \phi_0 \ \phi_1(\xi_{1,1}) \cdots \ \phi_1(\xi_{1,n}) \ \phi_2(\xi_{1,1}^2) \cdots \ \phi_2(\xi_{1,n}^2) \\ \phi_0 \ \phi_1(\xi_{2,1}) \cdots \ \phi_1(\xi_{2,n}) \ \phi_2(\xi_{2,1}^2) \cdots \ \phi_2(\xi_{2,n}^2) \\ \vdots \ \ddots \ \vdots \\ \phi_0 \ \phi_1(\xi_{S,1}) \cdots \ \phi_1(\xi_{S,n}) \ \phi_2(\xi_{S,1}^2) \cdots \ \phi_2(\xi_{S,n}^2) \end{bmatrix},$$
(24)

and $\xi_{s,i}$ is the *i*th element of the *s*th sample; $A \in \mathbb{R}^{(2n+1)\times L}$ is the coefficient matrix

$$\mathbf{A} = \begin{bmatrix} a_0^{(1)} & a_0^{(2)} & \cdots & a_0^{(L)} \\ a_1^{(1)} & a_1^{(2)} & \cdots & a_1^{(L)} \\ \vdots & \vdots & \ddots & \vdots \\ a_n^{(1)} & a_n^{(2)} & \cdots & a_n^{(L)} \\ a_{1,1}^{(1)} & a_{1,1}^{(2)} & \cdots & a_{1,1}^{(L)} \\ \vdots & \vdots & \ddots & \vdots \\ a_{n,n}^{(1)} & a_{n,n}^{(2)} & \cdots & a_{n,n}^{(L)} \end{bmatrix},$$
(25)

and $a_0^{(l)}, a_i^{(l)}, and \, a_{i,i}^{(l)}$ stand for the polynomial chaos coefficients with respect to the ith input and lth output.

Based on the obtained basis and output matrices, the coefficient matrix is calculated through

$$A = H^{-1}Y. (26)$$

According to (20), the mean of the output variable is $\hat{y} = A_1 = [a_0^{(1)}, a_0^{(2)}, \dots, a_0^{(L)}]^\mathsf{T}$, and the covariance matrix of the output variable is given by $P_y = A_2^\mathsf{T} A_2$, where A_2 is the remaining $2n \times L$ block of A, reflecting the second-moment information.

The detailed gPC procedure is described in Algorithm 1.

Algorithm 1: gPC Procedure.

1: Map the *i*th random variable x_i to a given random variable ξ_i via

$$x_i = F_i^{-1}(T_i(\xi_i)), i = 1, 2, \dots, n,$$

where F_i^{-1} is the inverse cumulative distribution function of x_i , and T_i is the cumulative distribution function of ξ_i ;

- 2: Construct the polynomial chaos basis, then express the output *y* in the gPC expansion form of (21);
- 3: Choose combinations of collocation points and put them into the polynomial chaos basis matrix (24);
- 4: Compute the model output for the selected collocation points to obtain the output matrix **Y**;
- 5: Estimate the unknown coefficients *A* based on the collocation points selected and the model output calculated by (26).

IV. THE PROPOSED GPC-BASED OBSERVABILITY ANALYSIS APPROACH

In this section, using the aforementioned polynomial-chaos technique, we present the proposed derivative-free observability analysis approach. Since we consider a more general stochastic dynamical system (6) instead of the traditional deterministic system (1), let us first extend the concept of observability to a stochastic one as shown in the following.

Definition 2: A stochastic system is (locally) observable in the time interval [0, K] if the initial state x_0 can be inferred from the measurements y_k , $k \in [0, K]$ and its solution satisfies a certain confidence interval level.

Now, within this stochastic framework, let us illustrate the proposed gPC-based observability analysis method.

A. Observability Condition

For the power system model described in (7)–(18), let us use a surrogate model to represent the relation between the arbitrary initial state x_k and its corresponding measurements Y_k by

$$\boldsymbol{Y}_k = \boldsymbol{H}\boldsymbol{A}_k. \tag{27}$$

In the surrogate model, since the means of the first-order and second-order polynomial chaos bases are zeros due to the orthogonal property [16], the zeroth-order polynomial chaos basis and its corresponding polynomial chaos coefficient $(a_0^{(l)}\phi_0)$ denote the mean of the lth measurement, and the first- and the second-order polynomial chaos bases and their corresponding polynomial chaos coefficients $(a_i^{(l)}\phi_1(\xi_{s,i}))$ and $a_{i,i}^{(l)}\phi_2(\xi_{s,i}^2))$ represent the uncertainty of the lth measurement with respect to the uncertainty of the ith state, where $\phi_1(\xi_{s,i})$ and $\phi_2(\xi_{s,i}^2)$ denote the first- and second-order polynomial chaos bases associated with the ith state, respectively. Further, the polynomial chaos coefficients, $a_i^{(l)}$ and $a_{i,i}^{(l)}$, stand for the contribution of the ith state to the uncertainty of the lth measurement.

When the contribution of the ith state to the uncertainty of the lth measurement is zero, it means that the value of the lth measurement remains unchanged with respect to the variations in this state, i.e., the ith state cannot be inferred from the lth measurement. To infer the n states from the given measurements uniquely, n effective measurements, for which the contributions of the states to the uncertainties of the measurements are linearly independent, are needed. That is, the observability-coefficient matrix, $\Phi_k \in \mathbb{R}^{2n \times mn}$,

$$\Phi_{k} = \begin{bmatrix}
a_{1}^{(1)} & a_{1}^{(2)} & \cdots & a_{1}^{(mn)} \\
\vdots & \vdots & \ddots & \vdots \\
a_{n}^{(1)} & a_{n}^{(2)} & \cdots & a_{n}^{(mn)} \\
a_{1,1}^{(1)} & a_{1,1}^{(2)} & \cdots & a_{1,1}^{(mn)} \\
\vdots & \vdots & \ddots & \vdots \\
a_{n,n}^{(1)} & a_{n,n}^{(2)} & \cdots & a_{n,n}^{(mn)}
\end{bmatrix},$$
(28)

which is the submatrix of the coefficient matrix, has n linearly independent columns, and the ith and (n+i)th rows cannot be zeros

Theorem 2: The system (1) is (locally) observable if and only if the observability-coefficient matrix Φ_k has n linearly independent columns and the ith and (n+i)th rows cannot be all zeros.

B. Degree of Observability

Since the extended definition of the observability of a stochastic dynamical system introduced in *Definition 2* also focuses on the confidence of the solution, we would like to further propose two new quantitative observability indices to measure the degree of observability from three aspects.

1) Contribution Rate: According to the surrogate model, the variance of the *l*th measurement can be determined via

$$\sigma_y^{2(l)} = \sum_{i=1}^n a_i^{2(l)} + a_{i,i}^{2(l)}, \tag{29}$$

where $\{a_i^{2(l)}+a_{i,i}^{2(l)}\}$ denotes the contribution of the ith state to the variance of the lth measurement.

Define the proportion of the contribution of the *i*th state to the variance of the *l*th measurement as the *contribution rate*, as

$$Q_i^{(l)} = \frac{a_i^{2(l)} + a_{i,i}^{2(l)}}{\sigma_u^{2(l)}}. (30)$$

It follows that $0 \leq Q_i^{(l)} \leq 1$. The contribution rate denotes the influence of the state on the measurement. A larger contribution rate implies a larger influence of the state on the measurement, and vice versa.

Definition 3: if all the contribution rates $(Q_i^{(1)},Q_i^{(2)},\ldots,Q_i^{(mn)})$ of the *i*th state are less than a small positive value (e.g., 0.1%), that state is *puny* observable. Otherwise, it is brawny observable. If all the states are *brawny* observable, the system is brawny observable. Otherwise, the system is puny observable.

2) Numerical Stability: To guarantee the numerical stability of the estimated state, the observability-coefficient matrix must be well-conditioned. The condition number, which is the ratio of the largest singular value to the smallest one, i.e.,

$$c(\mathbf{\Phi}) = \frac{\sigma_{\max}(\mathbf{\Phi})}{\sigma_{\min}(\mathbf{\Phi})} \tag{31}$$

is used to evaluate the matrix.

Definition 4: If the condition number is very large or becomes infinity, the system is puny observable. If the condition number is close to one, the system is brawny observable.

3) Interference Rate: Our approach can also assess the effect of observation noise on system observability.

If the contribution of the ith state (given by $a_i^{2(l)} + a_{i,i}^{2(l)}$) to the variance of the lth measurement is close to or smaller than the measurement noise variance, $\sigma_v^{2(l)}$, its influence is difficult to distinguish from that of the noise variance.

Define the proportion of the noise variance to the variance of the *l*th measurement as the *interference rate*, i.e.,

$$V^{(l)} = \frac{\sigma_v^{2(l)}}{\sigma_z^{2(l)}}. (32)$$

Definition 5: For a noisy measurement environment, the ith state is puny observable when all the contribution rates $(Q_i^{(1)}, Q_i^{(2)}, \dots, Q_i^{(mn)})$ are less than the corresponding interference rates $(V^{(1)}, V^{(2)}, \dots, V^{(mn)})$.

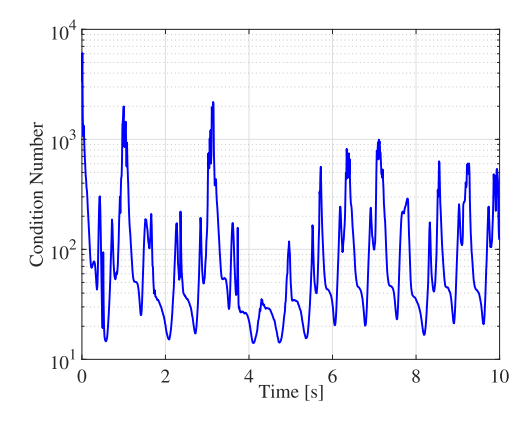


Fig. 1. Lie-derivative-based approach: condition number of the observability matrix.

Till now, we have presented the proposed gPC-based observability analysis method. Next, its performance will be assessed using some simulation results.

V. SIMULATION RESULTS

Here, let us first show a simple demonstration using the Lorenz system. Then, we will further validate the proposed method in a more complicated synchronous generator model with the IEEE-DC1A exciter and the TGOV1 turbine-governor.

A. Demonstration With a Lorenz System

Here, let us conduct a demonstration of the proposed method on the well-known Lorenz system, which is a typical nonlinear, chaotic system. Its system model is described by

$$\begin{cases} \dot{x}_1 = -10x_1 + 10x_2 \\ \dot{x}_2 = 28x_1 - x_1x_3 - x_2 \\ \dot{x}_3 = x_1x_2 - \frac{8}{3}x_3 \end{cases}$$
 (33)

with the initial states $\dot{x}_1=\dot{x}_2=\dot{x}_3=1$. Its measurement model is set to

$$\begin{cases} y_1 = x_1 \\ y_2 = x_2 \end{cases} \tag{34}$$

- 1) Lie-Derivative-Based Observability Analysis Approach: The observability analysis is first performed by using the Lie-derivative-based approach. The observability matrix is calculated and it has full rank at all times, which means that the system is observable. To measure the degree of the observability, the condition number is considered, as shown in Fig. 1. It shows that its value changes drastically and reaches large values at intervals, which reveals that the system is weakly observable. Note that the Lie-derivative-based approach can neither quantify the degree of observability for each state nor account for the effect of the observation noise, thereby reducing its reliability in practice.
- 2) Empirical Observability Gramian Approach: Observability analysis is then performed via the empirical observability Gramian approach. It consists of checking if the calculated observability matrix has full rank at all times, and deciding whether that is the case, i.e., that the system is observable. To

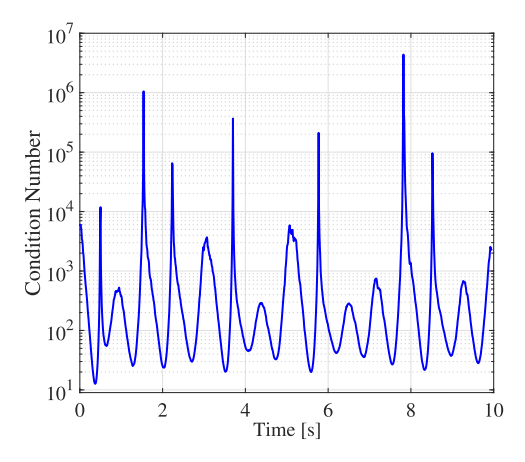


Fig. 2. Empirical observability Gramian approach: condition number of the observability matrix.

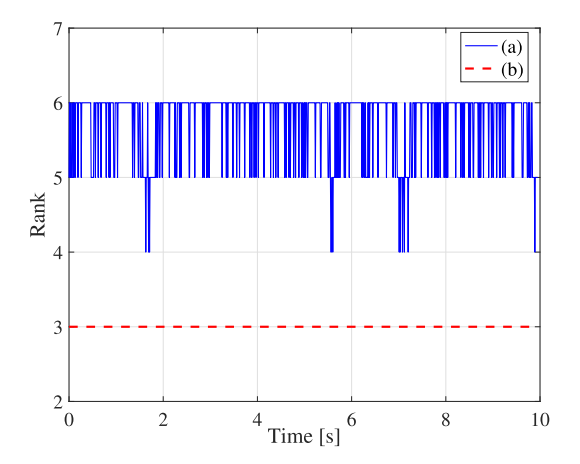


Fig. 3. gPC-based approach—rank of the matrices: (a) the observability-coefficient matrix and (b) the first-order coefficient matrix.

measure the degree of the observability, the condition number is calculated as shown in Fig. 2. It is observed that its value changes drastically and reaches large values at intervals, which reveals that the system is weakly observable. Hence, similar to the Liederivative-based approach, the empirical observability Gramian approach can neither quantify the degree of observability for each state nor account for the effect of the observation noise, thereby having some limitations in practice.

3) gPC-Based Approach: Here, we perform the observability analysis by using our gPC-based approach, in which the observability-coefficient matrix is computed through (28). In the observability-coefficient matrix, the first-order polynomial chaos coefficients are much larger than the second-order polynomial chaos coefficients. For the convenience of illustration, we define a matrix composed of the first-order polynomial chaos coefficients (i.e., the first n rows of the observability-coefficient matrix) and name it the first-order coefficient matrix.

First, let us test the observability condition using the rank of the observability-coefficient matrix as shown in Fig. 3(a). It is shown that the observability-coefficient matrix cannot be full rank at all times. However, as shown in Fig. 3(b), the first-order coefficient matrix has full rank all the time, which satisfies the observability condition. Hence, the system is observable.

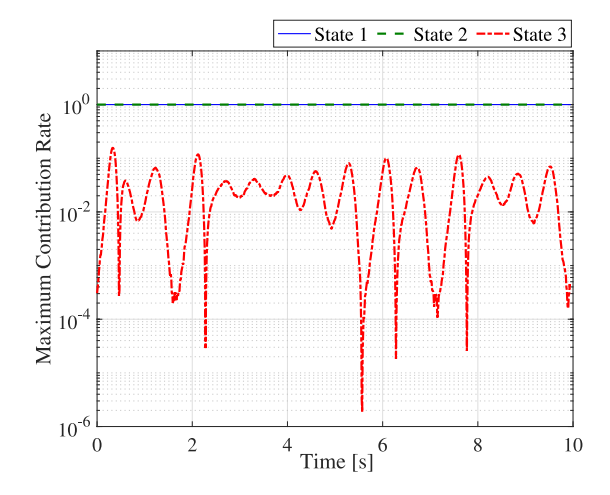


Fig. 4. gPC-based approach: maximum contribution rate.

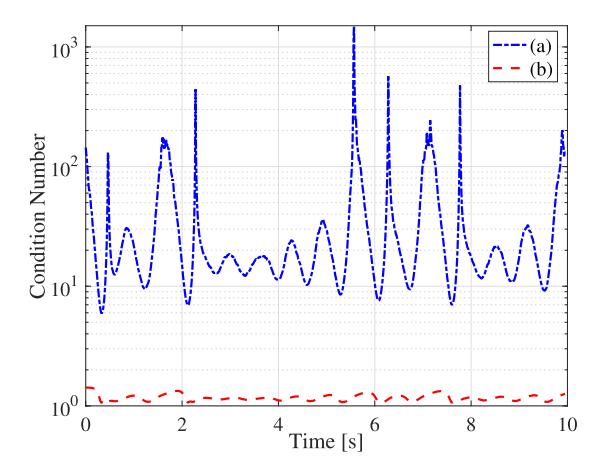


Fig. 5. gPC-based approach—condition number of the matrices: (a) the first-order coefficient matrix and (b) the active coefficient matrix.

Next, let us discuss the degree of observability. The contribution rate is considered first with its maximum contribution rate shown in Fig. 4, where the maximum contribution rate $Q_i^{\max}(t)$ of the ith state at time t is the maximum value of the contribution rates to the measurements. As can be seen, unlike the first two states with larger contribution rates (equal to one), the contribution rate of the third state varies with the time. For some time periods, it even reaches a very small value, rendering it hard to be inferred. Therefore, the first two states are brawny observable while the third state is puny observable.

Let us now show that the condition number of the observability-coefficient matrix can sometimes be very large. The condition number of the first-order coefficient matrix is displayed in Fig. 5(a). We observe that it varies with time while taking large values, indicating ill-conditioned conditions. Consequently, the state estimate is not numerically stable, which is also indicated in the contribution rate. For the sake of convenience, we define a matrix composed of the first-order polynomial chaos coefficients of the states with brawny observability, and call it the *active* coefficient matrix. The condition number of the active coefficient matrix is demonstrated in Fig. 5(b). It shows that the condition number of the active coefficient matrix is small enough to ensure that the active coefficient matrix

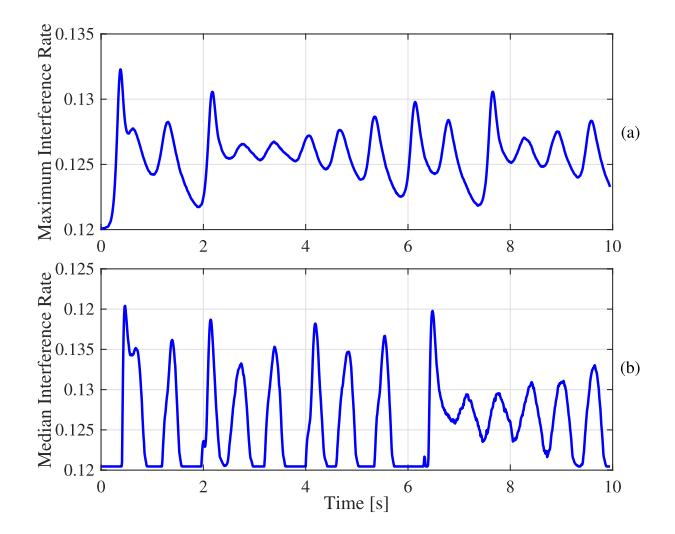


Fig. 6. gPC-based approach—interference rate: (a) maximum interference rate when the variance of the observation noise is 1×10^{-4} ; and (b) median interference rate when the variance of the observation noise is 1×10^{-2} .

is well-conditioned, which means the first two states can be well-estimated.

Now, let us investigate the effect of the observation noise on the observability of the dynamical system. The noise variance is 1×10^{-4} . Define the maximum interference rate, $V^{(l)}(t)$, at time t as the maximum value of the interference rates to the measurements, as shown in Fig. 6(a). It is noticeable that the maximum interference rate is too small to have an impact on the measurement. Hence, the effect of the observation noise on the state estimation is negligible. Moreover, we consider a noisy environment, where the noise variance is 1×10^{-2} . Define the median interference rate, $V^{(l)}(t)$, at time t as the median value of the interference rates to the measurements, as shown in Fig. 6(b). As can be seen, the median interference rate is very large, which indicates that most of the variances of the estimated values for the measurements are smaller than the variance of the observation noise. The states are hard to be inferred from the measurements since their influence is difficult to be distinguished from that of the noise variance. Therefore, the estimated results are heavily impacted by the observation noise, implying that the system is puny observable.

Finally, the effectiveness of the observability analysis result is verified through a DSE by using the unscented Kalman filter (UKF) [2]. The performance of the dynamic state estimator is evaluated by the root-mean-square error (RMSE). Four types of the implementations are considered. The first one performs the state estimation with the complete state prediction and the state-correction procedures, as shown in Fig. 7(a). In the second implementation, the state correction of the third state with puny observability is canceled, as shown in Fig. 7(b). In the third implementation, the state corrections of both the second and third states are canceled, as shown in Fig. 7(c). In the last implementation, the state estimation is performed under a noisy environment, as shown in Fig. 7(d). Obviously, the dynamic state estimation results obtained from the first two implementations

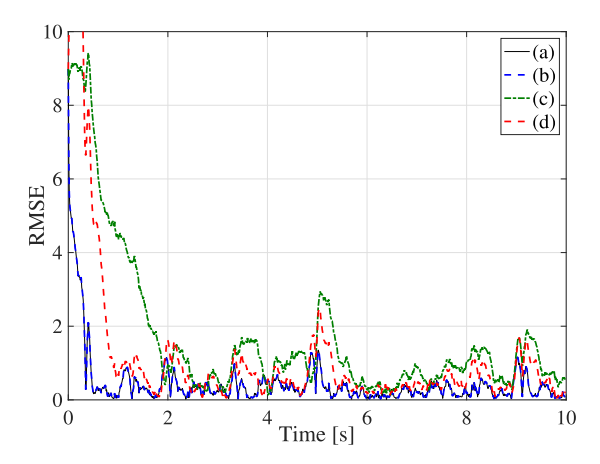


Fig. 7. RMSE: (a) the state estimation is performed with the complete state propagation and the state correction (the variance of the observation noise is 1×10^{-4}); (b) the state correction of the third state is canceled (the variance of the observation noise is 1×10^{-4}); (c) the state corrections of both the second and third states are canceled (the variance of the observation noise is 1×10^{-4}); and (d) the state estimation is performed with the complete state propagation and the state correction (the variance of the observation noise is 1×10^{-2}).

TABLE I COMPUTATION TIME OF APPROACHES

Approach	Computation Time [s]
Lie-derivative-based approach	13.2 ± 0.5
Empirical observability Gramian approach	0.86 ± 0.08
gPC-based approach	$0.058 \pm 0.0.005$

are the same, and they match the true states very well. In the second implementation, although the third state is puny observable (i.e., they are hard to be inferred from the measurements), they can be estimated through the state propagation with good state initialization. As demonstrated in the third implementation, the state estimation becomes worse when the state correction of the second state is also canceled. In the last implementation, due to the effect of the observation noise, the state estimates fluctuate around the true states, which result in a larger estimation error.

In this demonstration, we have clearly demonstrated that the proposed method is much more informative regarding the observability analysis than the traditional deterministic one.

4) Computation Time: The computational complexity is evaluated through computation time in Table I. The computation time is measured by using MATLAB R2017a on a 3.20-GHz Intel CoreTM i7 processor with a 8 GB of main memory. It is evident that our gPC-based approach takes much less computation time than the Lie-derivative-based method (i.e., a speedup of two orders of magnitude) in this nonlinear, chaotic system.

B. Decentralized DSE Case

In this section, an observability analysis for decentralized DSE is performed by using our approach. As a benchmark system, the IEEE 10-machine, 39-bus system is considered, and the synchronous generator is modeled by a ninth-order two-axis model with the IEEE-DC1A exciter and the TGOV1 turbine-governor. The sampling rate of the PMU is assumed to be 60 samples/s. A disturbance is applied at $t=0.5\,\mathrm{s}$ by opening the transmission line between Buses 15 and 16.

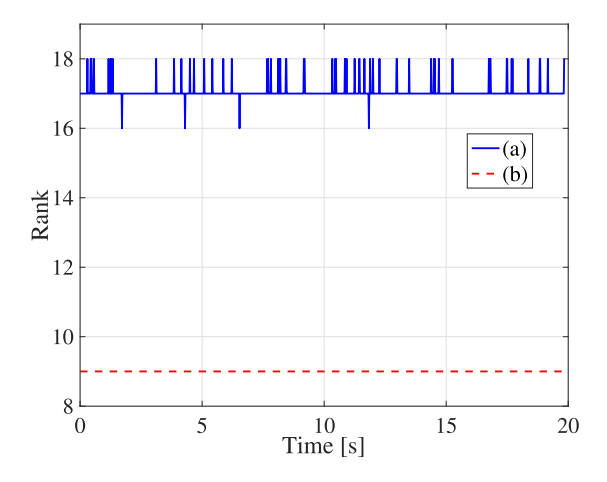


Fig. 8. Decentralized framework—rank of the matrices for the general case: (a) the observability-coefficient matrix, (b) the first-order coefficient matrix.

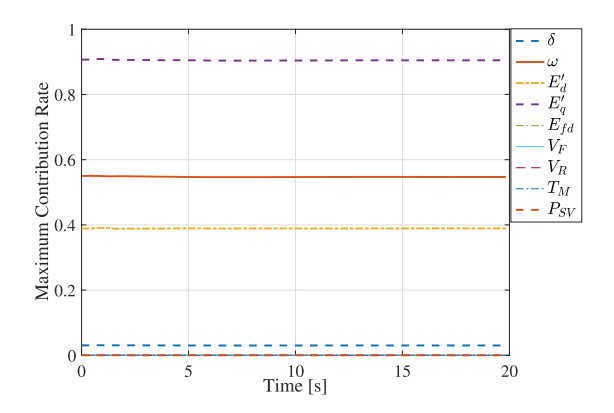


Fig. 9. Decentralized framework: maximum contribution rate for the general case.

1) General Test Case: Let us first consider a general case, in which both the real and reactive power are used as measurements for state estimation.

First, let us test the observability condition, for which the rank of the observability-coefficient matrix of the generator 5 is shown in Fig. 8(a). It is shown that the observability-coefficient matrix cannot have full rank all the time. However, as shown in Fig. 8(b), the first-order coefficient matrix has full rank all the time, which satisfies the observability condition. Hence, the system is observable.

Now, let us discuss the degree of observability, for which the maximum contribution rate is shown in Fig. 9. As can be seen, the first four states, i.e., δ , ω , E'_d , and E'_q , have the larger contribution rates, which means they can be more easily estimated with the given measurements while the other five states, i.e., E_{fd} , V_F , V_R , T_M , and P_{SV} , have negligible contribution rates, which implies that it is hard for them to be inferred from the given measurements. Therefore, the first four states are brawny observable while the other five states are puny observable.

Since the rank of the observability-coefficient matrix cannot have full rank all the time, the condition number of the observability-coefficient matrix can sometimes be very large. The condition number of the first-order coefficient matrix is demonstrated in Fig. 10(a). The condition number of the firstorder coefficient matrix varies with time while taking large

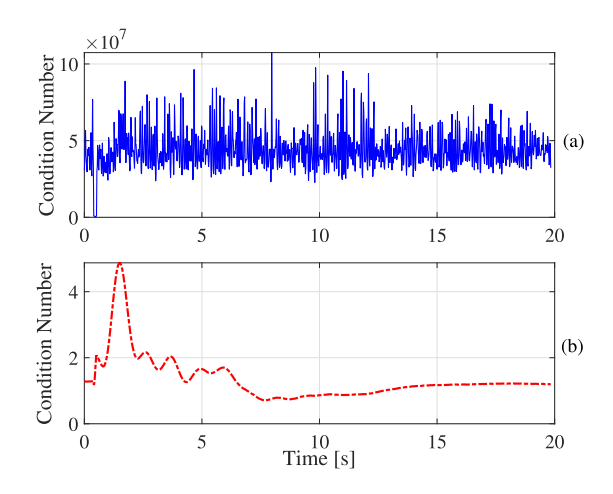


Fig. 10. Decentralized framework—condition number of the matrices for the general case: (a) the first-order coefficient matrix and (b) the active coefficient matrix.

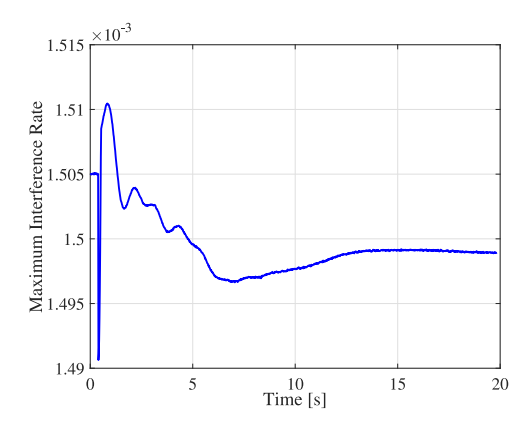


Fig. 11. Decentralized framework: maximum interference rate for the general case.

values that result in an ill-conditioned observability matrix. Consequently, the state estimate is not numerically stable, which is in agreement with the result obtained from the contribution rate. The condition number of the *active* coefficient matrix is demonstrated in Fig. 10(b). It shows that the condition number of the active coefficient matrix is small enough to ensure that the active coefficient matrix is well-conditioned, which means that the first four states can be well-estimated.

Finally, let us discuss the effect of the observation noise on the observability of this dynamical system. While considering the interference rate, the maximum interference rate is calculated and displayed in Fig. 11. Evidently, it is very small, which has only a negligible effect on the measurements. Hence, the effect of the observation noise on the state estimation is negligible.

The effectiveness of the observability analysis result is verified through a DSE. Due to space limitation, let us choose four brawny observable states (i.e., δ , ω , E'_d and E'_q) and two puny observable states (i.e., V_F and T_M) to demonstrate the effectiveness of the proposed approach.

The state estimation results are provided in Fig. 12. Three types of implementation are considered. The first one performs a state estimation with the complete state prediction and the state-correction procedures. The simulation results are displayed in Fig. 12(a), and its performance is indexed by the RMSE in

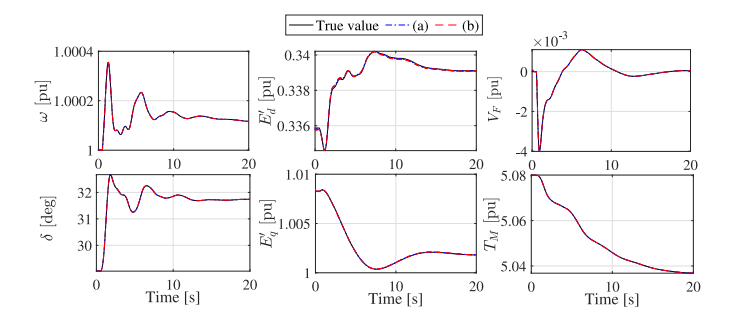


Fig. 12. Decentralized framework—state estimation results for the general case: (a) the state estimation is performed with the complete state propagation and the state correction; and (b) the state correction of the last five states is canceled.

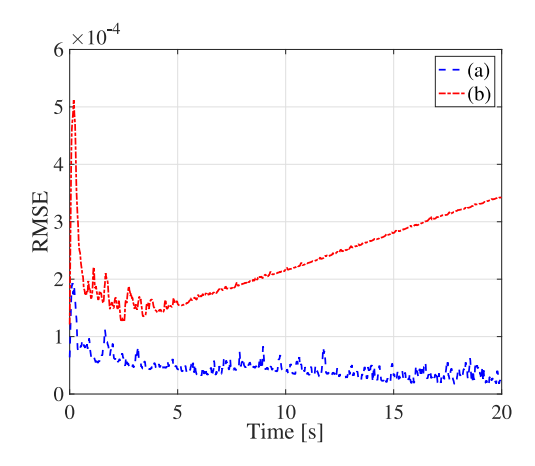


Fig. 13. Decentralized framework—RMSE for the general case: (a) the state estimation is performed with the complete state propagation and the state correction, and (b) the state corrections of the first four states are canceled.

Fig. 13(a). In the second implementation, the state corrections of the last five states with puny observability are canceled, as shown in Fig. 12(b). In the third implementation, the state corrections of the first four states are canceled, and it performance is indexed in Fig. 13(b).

As can be seen, the state estimation results obtained from the first two implementations are the same, and they match the true states very well. In the second implementation, although the last five states are puny observable (i.e., they are hard to be inferred from the measurements), they can be estimated through the state propagation with good state initialization. As demonstrated in the third implementation, the state estimation becomes worse when the state corrections of the first four states are canceled.

The state estimation under different initial state conditions is also studied in the simulations. A brawny observable state and a puny observable state are estimated and their trajectories are plotted in Fig. 14. Thanks to the effective state-correction process, the estimated state with brawny observability closely tracks the true state in the initial stage. However, since the state-correction process rarely works for the puny observable state, the estimated value converges to the true value very slowly.

2) Special Test Case: Now, let us further consider a special case to demonstrate the effectiveness of the proposed method. In this case, only the real power is used as the measurement while the reactive power is ignored. In this case, the observability-coefficient matrix is of full rank at all time steps, which means

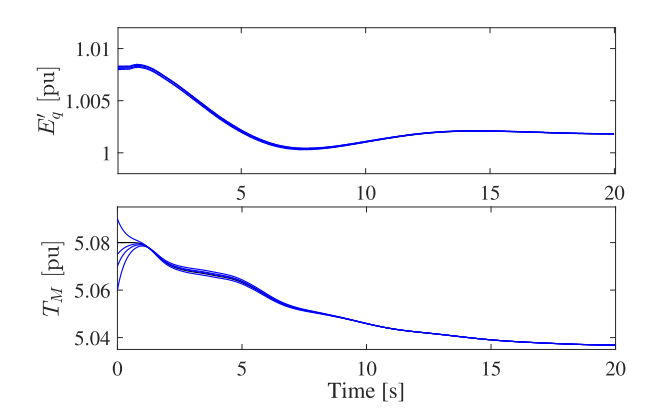


Fig. 14. Decentralized framework: state estimation results under different state initial conditions for the general case.

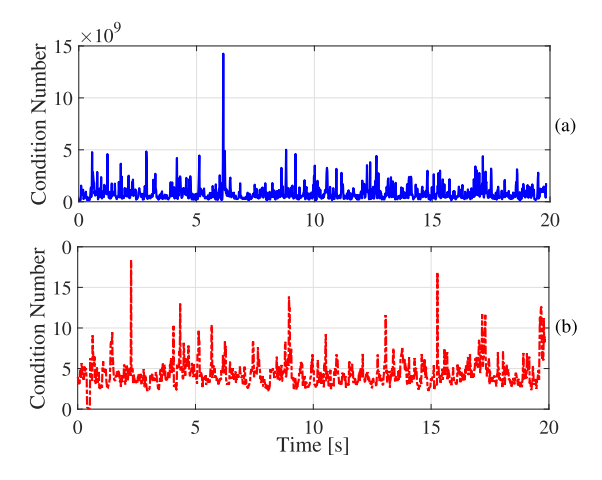


Fig. 15. Decentralized framework—condition number of the matrices for the special case: (a) the first-order coefficient matrix and (b) the active coefficient matrix.

that the system is observable. The maximum contribution rate is similar to that in Fig. 9, which indicates that the last five states are puny observable.

Since the rank of the observability-coefficient matrix cannot have full rank all the time, the condition number of the observability-coefficient matrix can sometimes be very large. The condition number of the first-order coefficient matrix is demonstrated in Fig. 15(a). The condition number of the firstorder coefficient matrix varies with time while taking large values that result in ill-conditioned observability matrix. Consequently, the state estimate is not numerically stable, which is in agreement with the result obtained from the contribution rate. The condition number of the active coefficient matrix is displayed in Fig. 15(b). It shows that the condition number of the active coefficient matrix takes large values, resulting in an ill-conditioned matrix. Hence, the first four states still suffer from numerical instability, which agrees with the result obtained by using the Lie-derivative-based observability analysis approach [11]. The estimation result of the decentralized DSE that only takes P_e as the measurement plotted in Fig. 16, which shows that the state estimates do not fully match the true values because they are not numerically stable. This further demonstrates the effectiveness of the proposed gPC-based observability analysis approach.

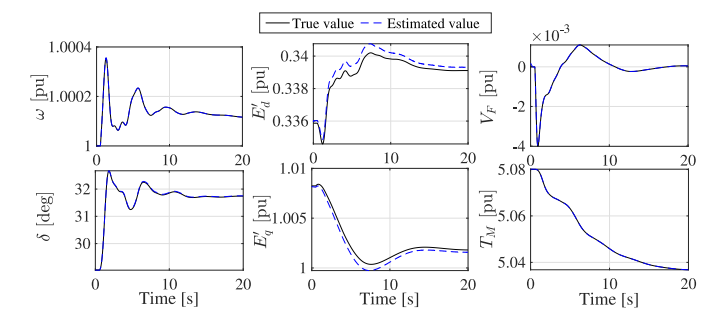


Fig. 16. Decentralized framework: state estimation results for the special case.

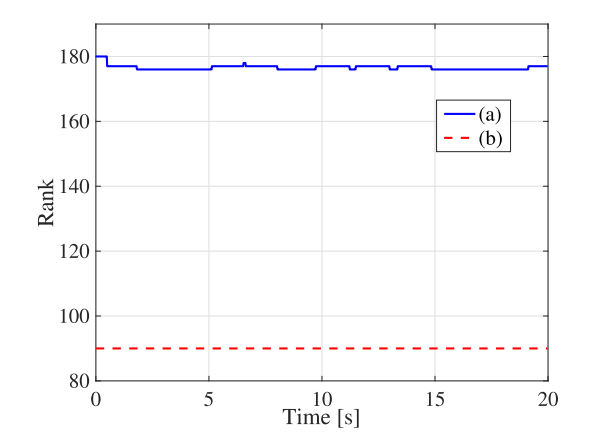


Fig. 17. Centralized framework—rank of the matrices: (a) the observability-coefficient matrix, and (b) the first-order coefficient matrix.

3) Computing Time: Finally, we should highlight that the entire observability analysis only takes around 0.21 s for the general case study and 0.17 s for the special case, which is compatible with online applications.

C. Centralized DSE Case

In this section, we consider a very challenging task to our approach by performing an observability analysis of a centralized DSE applied to the IEEE 10-machine, 39-bus system. Here, the synchronous generator is modeled by a ninth-order two-axis model with the IEEE-DC1A exciter and the TGOV1 turbine-governor. The other scenarios are the same as those of the decentralized case.

First, let us test the observability condition for which the rank of the observability-coefficient matrix is shown in Fig. 17(a). It is shown that the observability-coefficient matrix cannot have full rank all the time. However, as shown in Fig. 17(b), the first-order coefficient matrix has full rank all the time, which satisfies the observability condition. Hence, the system is observable.

Now, let us discuss the degree of observability, for which the maximum contribution rate is shown in Fig. 18. As can be seen, the first forty states, i.e., δ , ω , E'_d , and E'_q of each generator, have the larger contribution rates, which means they can be more easily estimated with the given measurements while the other fifty states, i.e., E_{fd} , V_F , V_R , T_M , and P_{SV} , of each generator, have negligible contribution rates, which implies that it is hard for them to be inferred from the given measurements. Therefore,

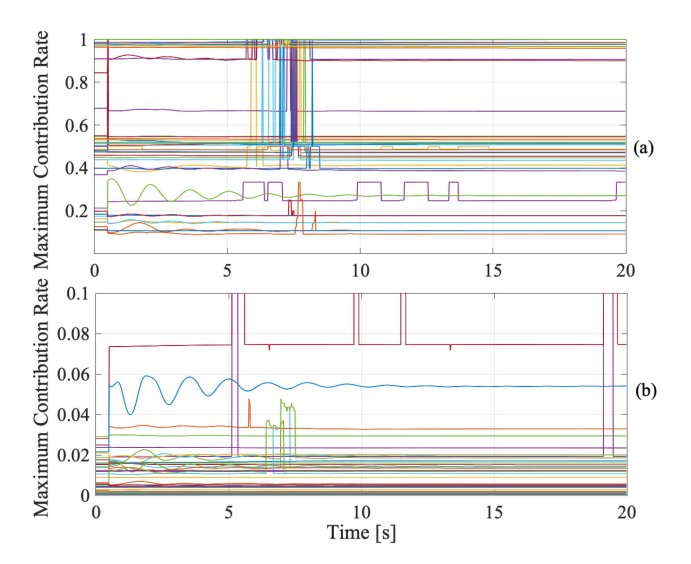


Fig. 18. Centralized framework—maximum contribution rate: (a) the first forty states and (b) the other fifty states.

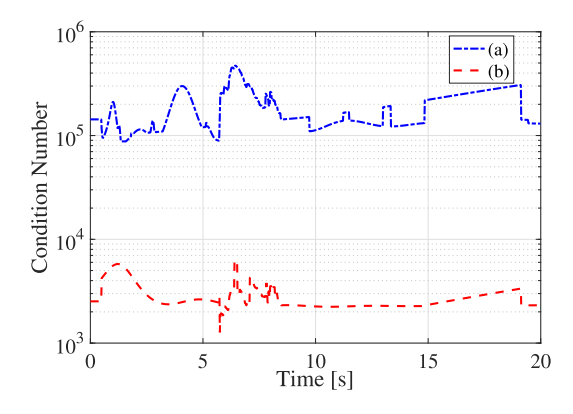


Fig. 19. Centralized framework—condition number of the matrices: (a) the first-order coefficient matrix and (b) the active coefficient matrix.

the first forty states are brawny observable while the other fifty states are puny observable.

Since the rank of the observability-coefficient matrix cannot have full rank all the time, the condition number of the observability-coefficient matrix can sometimes be very large. The condition number of the first-order coefficient matrix is shown in Fig. 19(a). It is observed that it varies with time while taking large values that result in an ill-conditioned observability matrix. Consequently, the state estimate is not numerically stable, which is in agreement with the result obtained from the contribution rate. The condition number of the *active* coefficient matrix is displayed in Fig. 19(b). It is observed that it is small enough to ensure that the active coefficient matrix is well-conditioned, which means that the first forty states can be well-estimated.

Now, let us investigate the effect of the observation noise on the observability of this dynamical system. The noise variance is 1×10^{-5} . While considering the interference rate, the median interference rate is calculated and displayed in Fig. 20(a). It is observed that the median interference rate is too small to impact the measurement. Hence, the effect of the observation noise on the state estimation is negligible. Now, let us consider a noisy

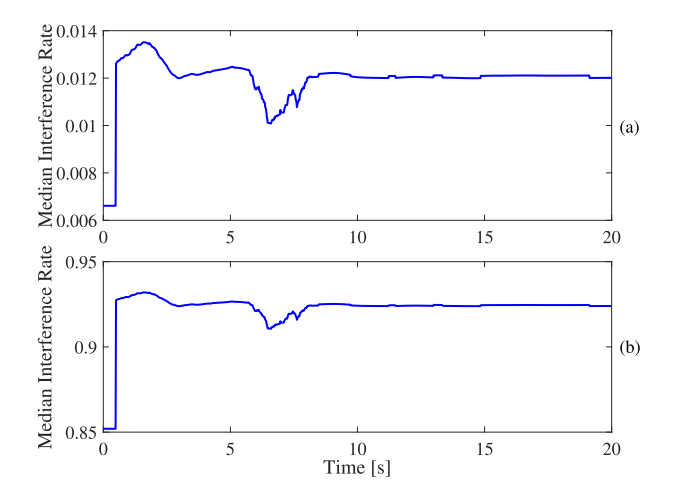


Fig. 20. Centralized framework—median interference rate: (a) the normal environment when the variance of the observation noise is 1×10^{-5} ; and (b) a noisy environment when the variance of the observation noise is 1×10^{-2} .

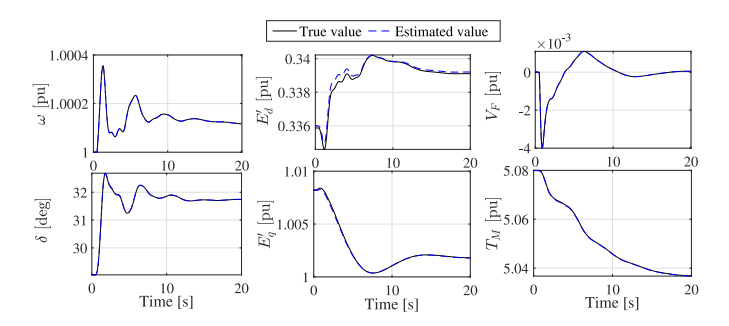


Fig. 21. Centralized framework: state estimation results for the normal environment.

environment where the noise variance is 1×10^{-2} . The median interference rate is displayed in Fig. 20(b). As can be seen, the median interference rate is very large, which indicates that most of the variances of the estimated values for the measurements are smaller than the variance of the observation noise. The states are hard to be inferred from the measurements since their influence cannot be easily distinguished from that of the noise variance. Therefore, the estimated results are heavily impacted by the observation noise, implying that the system is puny observable.

The effectiveness of the observability analysis result is demonstrated via a DSE. Here, two types of implementation are considered. The first one performs a state estimation in the normal environment, and the simulation results are displayed in Fig. 21. In the second implementation, the state estimation is performed under a noisy environment, as shown in Fig. 22. As can be seen, the state estimation results match the true states very closely in the first implementation. As demonstrated in the second implementation, due to the effect of the observation noise, the state estimates fluctuate around the true states, which results in a larger estimation error.

Finally, we need to highlight that the entire observability analysis only takes around 182.5 s, which is highly computationally efficient for such a large-scale dynamical power system with detailed generator model.

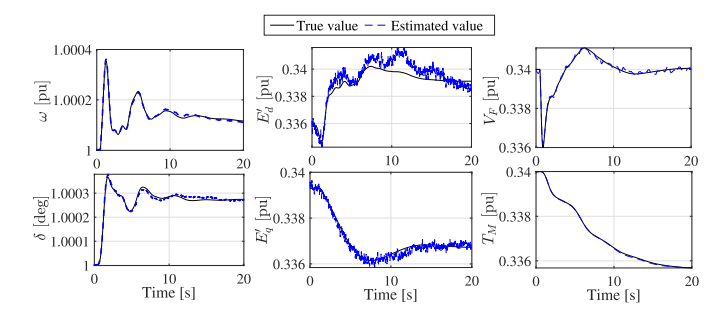


Fig. 22. Centralized framework: state estimation results for a noisy environment.

VI. CONCLUSION

In this paper, we propose a novel gPC-based derivative-free observability analysis approach for power system stochastic dynamic models. This method not only has a low complexity and an easy implementation, but also enables us to quantify the degree of observability. The excellent performances of the proposed method have been assessed in a number of simulations of power system DSE.

Our future work will involve using the gPC-based observability analysis tool to better design a DSE as well as sensor placement algorithms.

REFERENCES

- Z. Huang, P. Du, D. Kosterev, and S. Yang, "Generator dynamic model validation and parameter calibration using phasor measurements at the point of connection," *IEEE Trans. Power Syst.*, vol. 28, no. 2, pp. 1939–1949, May 2013
- [2] A. K. Singh and B. C. Pal, "Decentralized dynamic state estimation in power systems using unscented transformation," *IEEE Trans. Power Syst.*, vol. 29, no. 2, pp. 794–804, Mar. 2014.
- [3] Y. Guo, B. Zhang, W. Wu, and H. Sun, "Multi-time interval power system state estimation incorporating phasor measurements," in *Proc. IEEE Power Energy Soc. Gen. Meeting*, 2015, pp. 1–5.
- [4] J. Zhao et al., "Power system real-time monitoring by using PMU-based robust state estimation method," *IEEE Trans. Smart Grid*, vol. 7, no. 1, pp. 300–309, Jan. 2016.
- [5] M. Asprou, S. Chakrabarti, and E. Kyriakides, "A two-stage state estimator for dynamic monitoring of power systems," *IEEE Syst. J.*, vol. 11, no. 3, pp. 1767–1776, Sep. 2017.
- [6] N. M. Manousakis and G. N. Korres, "A hybrid power system state estimator using synchronized and unsynchronized sensors," *Int. Trans. Elect. Energy Syst.*, vol. 38, no. 8, Aug. 2018, Art no. e 2580.
- [7] J. Zhao et al., "Power system dynamic state estimation: Motivations, definitions, methodologies and future work," *IEEE Trans. Power Syst.*, vol. 34, no. 4, pp. 3188–3198, Jul. 2019.
- [8] S. A. Nugroho, A. F. Taha, and J. Qi, "Robust dynamic state estimation of synchronous machines with asymptotic state estimation error performance guarantees," *IEEE Trans. Power Syst.*, vol. 35, no. 3, pp. 1923–1935, May 2020.
- [9] J. Qi, K. Sun, and W. Kang, "Optimal PMU placement for power system dynamic state estimation by using empirical observability Gramian," *IEEE Trans. Power Syst.*, vol. 30, no. 4, pp. 2041–2054, Jul. 2015.
- [10] G. Wang, C. Liu, N. Bhatt, E. Farantatos, and M. Patel, "Observability of nonlinear power system dynamics using synchrophasor data," *Int. Trans. Elect. Energy Syst.*, vol. 26, no. 5, pp. 952–967, May 2016.
- [11] A. Rouhani and A. Abur, "Observability analysis for dynamic state estimation of synchronous machines," *IEEE Trans. Power Syst.*, vol. 32, no. 4, pp. 3168–3175, Jul. 2017.
- [12] P. W. Sauer and M. A. Pai, Power System Dynamics and Stability. Upper Saddle River, NJ, USA: Prentice-Hall, 1998.
- [13] S. G. Krantz and H. R. Parks, The Implicit Function Theorem: History, Theory, and Applications. New York, NY, USA: Springer Science Business Media, 2003.

- [14] C. T. Chen, Linear System Theory and Design. New York, NY, USA: Holt, Rinehart and Winston, 1984.
- [15] J. Zhao and L. Mili, "Power system robust decentralized dynamic state estimation based on multiple hypothesis testing," *IEEE Trans. Power Syst.*, vol. 33, no. 4, pp. 4553–4562, Jul. 2018.
- [16] D. Xiu and G. E. Karniadakis, "The Wiener-Askey polynomial chaos for stochastic differential equations," SIAM J. Sci. Comput., vol. 24, no. 2, pp. 619–644, 2002.
- [17] Y. Xu, L. Mili, A. Sandu, M. R. von Spakovsky, and J. Zhao, "Propagating uncertainty in power system dynamic simulations using polynomial chaos," *IEEE Trans. Power Syst.*, vol. 34, no. 1, pp. 338–348, Jan. 2019.
- [18] Y. Xu, L. Mili, and J. Zhao, "A novel polynomial-chaos-based Kalman filter," *IEEE Signal Process. Lett.*, vol. 26, no. 1, pp. 9–13, Jan. 2019.



Zongsheng Zheng (Member, IEEE) received the B.S. degree in bioinformatics and the Ph.D. degree in electrical engineering from Southwest Jiaotong University, Chengdu, China, in 2013 and 2020, respectively. During 2018–2019, he was a Visiting Scholar with the Bradley Department of Electrical and Computer Engineering, Virginia Tech-Northern Virginia Center, Falls Church, VA, USA. He is currently a Research Associate Professor with the College of Electrical Engineering, Sichuan University, Chengdu, China. His research interests include uncertainty quantification,

parameter, and state estimation.



Yijun Xu (Senior Member, IEEE) received the Ph.D. degree from the Bradley Department of Electrical and Computer Engineering, Virginia Tech, Falls Church, VA, USA, in December 2018. He is currently a Research Assistant Professor with Virginia Tech-Northern Virginia Center, Falls Church, VA, USA. During 2019–2020, he was a Postdoctoral Associate at same institute. He did the computation internship with Lawrence Livermore National Laboratory, Livermore, CA, USA, and power engineer internship with ETAP – Operation Technology, Inc., Irvine, CA,

USA, in 2018 and 2015, respectively.

His research interests include power system uncertainty quantification, uncertainty inversion, and decision-making under uncertainty. He is currently an Associate Editor for the *IET Generation, Transmission & Distribution*. He is the Co-Chair of the IEEE Task Force on Power System Uncertainty Quantification and Uncertainty-Aware Decision-Making.



Lamine Mili (Life Fellow, IEEE) received the Ph.D. degree from the University of Liège, Liège, Belgium, in 1987. He is currently a Professor of electrical and computer engineering with Virginia Tech, Blacksburg, VA, USA. He has five years of industrial experience with the Tunisian electric utility, STEG. At STEG, he was with Planning Department from 1976 to 1979 and then with the Test and Meter Laboratory from 1979 to 1981. He was a Visiting Professor with the Swiss Federal Institute of Technology Lausanne, Lausanne, Switzerland, the Grenoble Institute

of Technology, Grenoble, France, the École Supérieure D'électricité, France, and the École Polytechnique de Tunisie, Tunisia, and did consulting work for the French Power Transmission company, RTE.

His research interests include power system planning for enhanced resiliency and sustainability, risk management of complex systems to catastrophic failures, robust estimation and control, nonlinear dynamics, and bifurcation theory. He is the Co-Founder and the Co-Editor of the *International Journal of Critical Infrastructure*. He is the Chairman of the IEEE Working Group on State Estimation Algorithms and the Chair of the IEEE Task Force on Power System Uncertainty Quantification and Uncertainty-Aware Decision-Making. He was the recipient of several awards, including the US National Science Foundation (NSF) Research Initiation Award and the NSF Young Investigation Award.



Zhigang Liu (Senior Member, IEEE) received the Ph.D. degree in power system and its automation from the Southwest Jiaotong University, Chengdu, China, in 2003. He is currently a Full Professor with the School of Electrical Engineering, Southwest Jiaotong University. His research interests include the electrical relationship of EMUs and traction, detection, and assessment of pantograph-catenary in high-speed railway.

He has written three books, authored or coauthored more than 100 peer-reviewed journal and conference

papers. He was elected as a Fellow of The Institution of Engineering and Technology (IET) in 2017. He is an Associate Editor for the IEEE TRANSACTIONS ON NEURAL NETWORKS AND LEARNING SYSTEMS, IEEE TRANSACTIONS ON VEHICULAR TECHNOLOGY, IEEE TRANSACTIONS ON INSTRUMENTATION AND MEASUREMENT, and IEEE ACCESS. He was the recipient of the IEEE TIM's Outstanding Associate Editors for 2019 and 2020 and the Outstanding Reviewer of IEEE Transactions on Instrumentation and Measurement 2018.



Mert Korkali (Senior Member, IEEE) received the Ph.D. degree in electrical engineering from Northeastern University, Boston, MA, USA, in 2013. He is currently a Research Staff Member with Lawrence Livermore National Laboratory, Livermore, CA, USA. From 2013 to 2014, he was a Postdoctoral Research Associate with the University of Vermont, Burlington, VT, USA.

His current research interests include the broad interface of robust state estimation and fault location in power systems, cascading failures, uncertainty quan-

tification, and decision making under uncertainty. He is the Co-Chair of the IEEE Task Force on Standard Test Cases for Power System State Estimation and the Secretary of the IEEE Task Force on Power System Uncertainty Quantification and Uncertainty-Aware Decision-Making. He is currently the Editor of the IEEE OPEN ACCESS JOURNAL OF POWER AND ENERGY and of the IEEE POWER ENGINEERING LETTERS, and an Associate Editor of *Journal of Modern Power Systems and Clean Energy*.



Yuhong Wang (Member, IEEE) received the Ph.D. degree in power system and its automation from Southwest Jiaotong University, Chengdu, China, in 2008. She is currently a Professor with the College of Electrical Engineering, Sichuan University, Chengdu, China. From 1996 to 2004, she worked at Southwest Electric Power Design Institute as an engineer in charge of power system planning, and worked in Siemens AG Erlangen, Germany for Guiguang HVDC system design in 2002. She was a Visiting Professor with the Department of Electrical Engineering

and Computer Science, Massachusetts Institute of Technology, Cambridge, MA, USA from 2014 to 2015, Arizona State University, Tempe, AZ, USA, in 2011, and Technische Universitaet Clausthal, Germany, in 2017.

Her research interests include power system stability and control, high voltage direct current transmission system, renewable energy sources integration. She is currently a Member of PES, CEng. of The Institution of Engineering and Technology (IET).